Electronic Supplementary Material (ESI) for Nanoscale.
This journal is © The Royal Society of Chemistry 2022

Supplementary Material

Correlation of crystal structure and ion storage behavior of MoO_3 electrode materials for aluminum-ion energy storage studied with in-situ X-ray spectroscopies

Feng Hao Hsu, Su Yang Hsu‡, Bo Hao Chen, Jeng Lung Chen, Jin Ming Chen*,

Kueih Tzu Lu*

National Synchrotron Radiation Research Center, Hsinchu, 30076, Taiwan

*Authors to whom correspondence should be addressed. E-mail: jmchen@nsrrc.org.tw (J.M. C.) and ktlu@nsrrc.org.tw (K. T. Lu)

‡ Contributed equally to this work with first author: F. H. Hsu

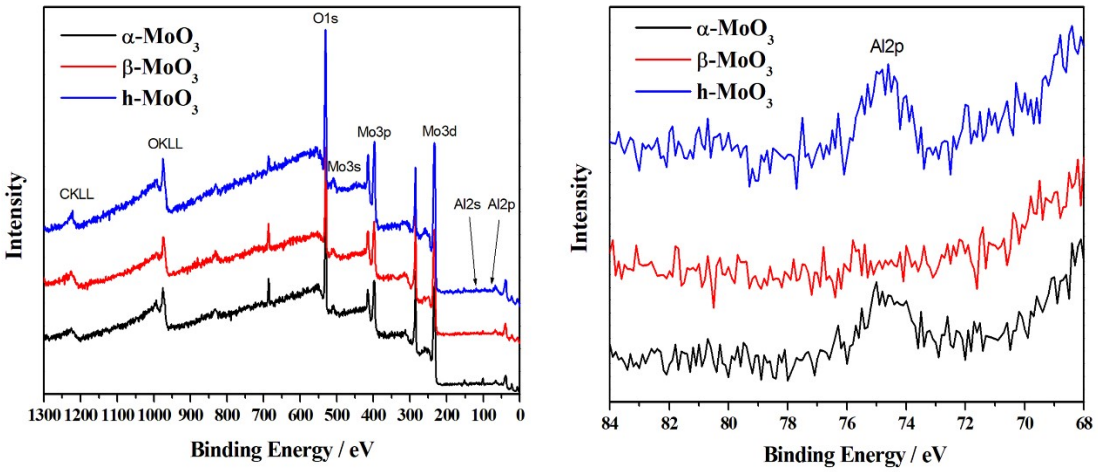

Figure S1. The XPS spectra of the MoO_3 materials with various crystal phases after insertion of Al^{3+} ion.

Table S1. As-characterized composition of the MoO_3 electrodes with various crystal phases after insertion of Al^{3+} ion deduced by XPS measurements.

Sample	Al atomic content %	Mo atomic content %	O atomic content %
α-MoO_3	1.33	19.07	79.59
β-MoO_3	0.14	21.92	77.94
h-MoO_3	0.98	20.99	78.09

The Electrochemical impedance spectroscopy (EIS) measurements of the various MoO_3 electrode materials are shown in Figure S2. The EIS measurements were recorded in a frequency range of 10^5 to 0.1 Hz at an open circuit potential. In the high-frequency region of Nyquist plots, the intersection with real axis and the diameter of semicircle represent the resistance of electrochemical system (R_s) and charge transfer resistance (R_{ct}), respectively. There clearly show smaller R_{ct} for the α-MoO_3 and h-MoO_3 electrode materials, whereas the β-MoO_3 electrode material has the largest R_{ct}. This result indicates that the charge-transfer at the interface for the α-MoO_3 and h-MoO_3 electrode materials is relatively easier than that for β-MoO_3. Furthermore, the slope of straight line in the low-frequency region is defined as the diffusion resistance. The slope trend (α-MoO_3 > h-MoO_3 and β-MoO_3) indicates that the diffusion resistance of α-MoO_3 is lower than that of h-MoO_3 and β-MoO_3, whereas the diffusion resistances of both h-MoO_3 and β-MoO_3 electrode materials show no significant difference.

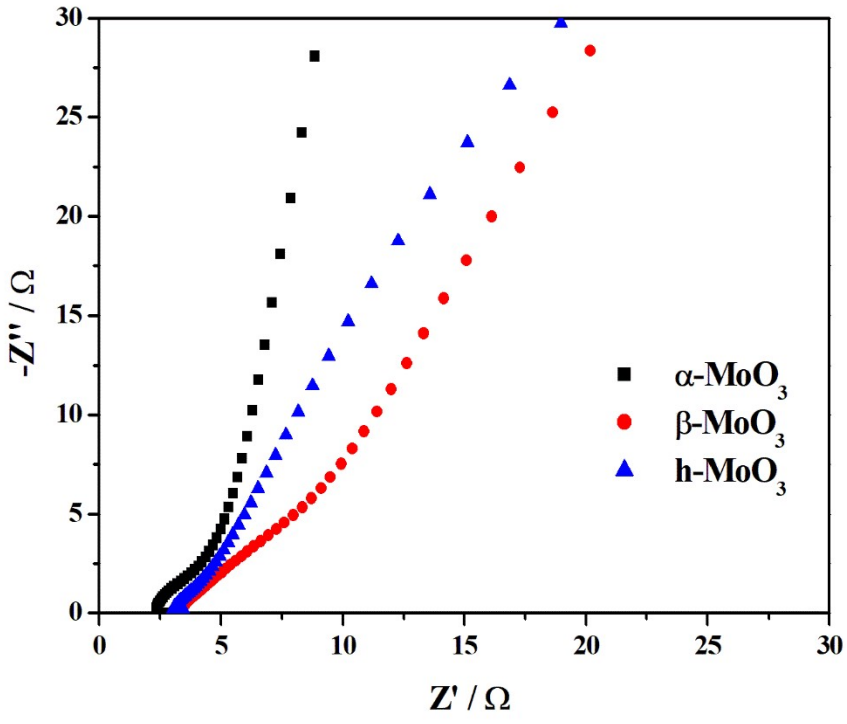

Figure S2. The EIS curves of various MoO_3 electrode materials.

The rate performance of the various MoO_3 electrode materials is characterized under current density from 1 A g^{-1} to 5 A g^{-1} with potential range from -0.7 V to 0.6 V. It is obseved that the charge and discharge gravimetric capacities are decreased with increasing current density, which is attributed to the polarization phenomenon of the MoO_3 electrode materials.

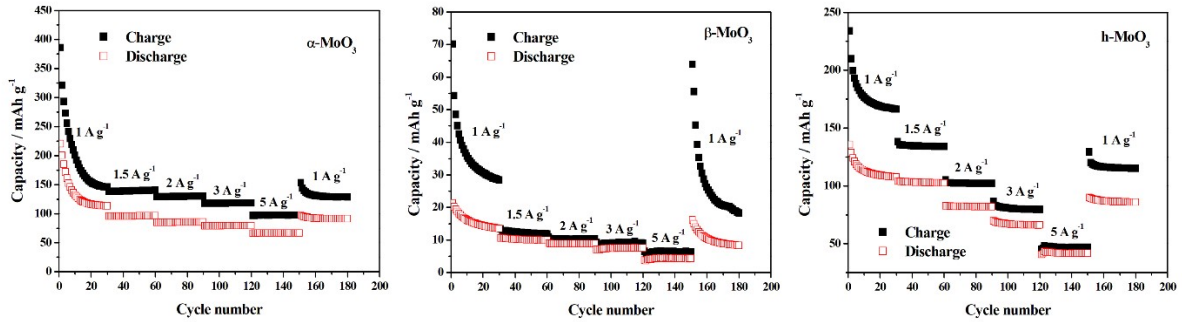

Figure S3. Rate performance and variation of charge/discharge capacities of the various MoO_3 electrode materials.

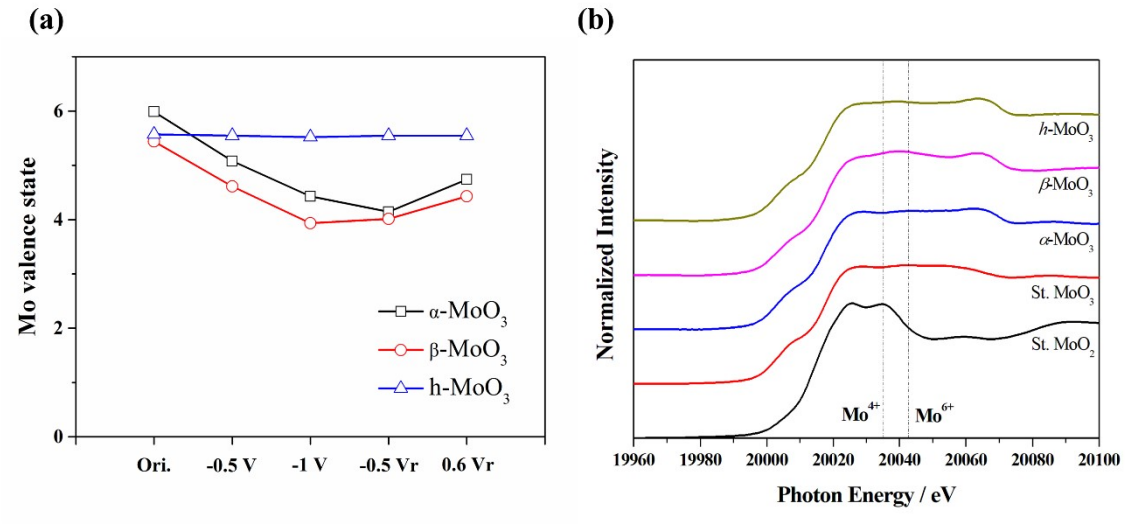

Figure S4. (a) The average valence state of Mo in the various MoO_3 electrode materials under insertion/extraction of Al^{3+} ion, and (b) the Mo K-edge XANES spectra of the various MoO_3 electrode materials together with the reference samples.

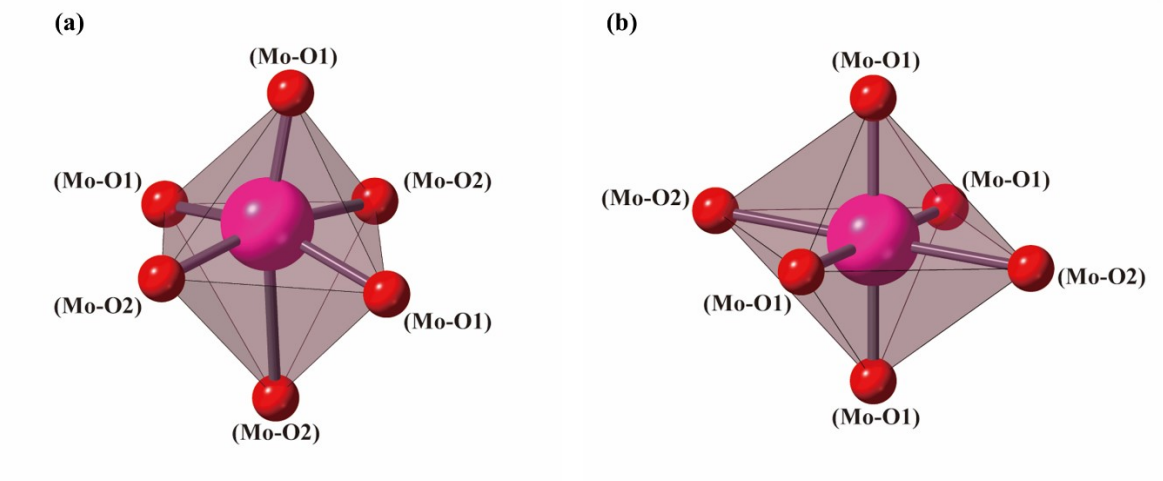

Figure S5. The MoO_6 octahedral structure in the (a) α-MoO_3, and (b) β-MoO_3 materials.